PHYSICAL REVIEW E **74**, 041901 (2006)

Electrophoresis of a polyelectrolyte through a nanopore

Sandip Ghosal*
Department of Mechanical Engineering, Northwestern University, Evanston, Illinois 60208, USA

(Received 26 June 2006; published 2 October 2006)

A hydrodynamic model for determining the electrophoretic speed of a polyelectrolyte through a nanopore is presented. It is assumed that the speed is determined by a balance of electrical and viscous forces arising from within the pore and that classical continuum electrostatics and hydrodynamics may be considered applicable. An explicit formula for the translocation speed as a function of the pore geometry and other physical parameters is obtained and is shown to be consistent with experimental measurements on DNA translocation through nanopores in silicon membranes. Experiments also show a weak dependence of the translocation speed on polymer length that is not accounted for by the present model. It is hypothesized that this is due to secondary effects that are neglected here.

DOI: 10.1103/PhysRevE.74.041901 PACS number(s): 87.15.Tt

Electrically driven translocation of DNA across natural and artificial nanopores can be detected on the single-molecule level by observing the increase of electrical resistance of the pore during such events [1]. Nanoscale pores may be fabricated by the self-assembly of the natural protein α-hemolysin on a lipid bilayer membrane [2,3] or by annealing a microfabricated hole in a Si/SiO_2 substrate using an intense electron beam from a transmission electron microscope (TEM) [4]. The setup for detecting the translocation events consists of a reservoir containing an electrolyte that is partitioned into two chambers by a membrane with the nanometer-scale pore forming the only communication between the two sides. An electrical potential difference is applied across the membrane, and the resulting current is monitored. The passage of a DNA strand is signaled by a drop in the current. The duration and amount of these dips in the current contain signatures of the DNA such as its length and base sequence. Possible applications of the technique to rapid DNA sequencing is being explored [3].

Lubensky and Nelson [5] provided an interpretation of some of the features of the experimental work cited above. In particular, they proposed a drift diffusion equation for $P(s,t)$: the probability that the DNA is found to have a length s on a given side of the partition at time t. This equation was shown to explain qualitatively the shape of the observed distribution of translocation times. It was presumed that the drift velocity itself is determined by a resistive force that opposes the electrical driving force, but the exact physical nature of this resistive force remained unclear. Viscous resistance could be a reasonable contender for a resistive force localized around the nanopore, but a simple estimate appeared to indicate that its value was orders of magnitude smaller than what was required.

Polymer translocation across nanopores driven by a variety of physical mechanisms have a number of other applications in biology; the injection of DNA from a virus into a host cell is a particularly interesting example [6]. These problems have been addressed by a number of authors [7–13] by formulating the problem in a probabilistic setting as a transition between two states separated by a barrier in the configurational entropy of the polymer chain. In all cases, the hydrodynamic resistance of the pore, when considered at all, is simply parametrized by a resistance coefficient. Most of the theoretical investigations of the subject to date are devoted to understanding how the translocation time of a polymer scales with polymer length, the scaling exponent being a quantity that may be expected to be independent of details such as the pore resistance and therefore amenable to experimental verification.

In this paper, we explicitly determine the translocation time by actually solving a simple hydrodynamic model for the translocation of a polymer through a water-filled pore. Translocation speeds are calculated and compared with the experimental data of Storm *et al.* [14] for solid-state nanopores.

Figure 1 is a sketch of the setup that also helps to explain our notation. The pore is assumed to be cylindrically symmetric[1] about the z axis and described by a function $R(z)$ that gives the distance to the wall of the pore from the axis at any z location. The part of the polyelectrolyte within the pore is modeled as a straight cylinder of radius a and carrying a uniform charge of density λ per unit length. The length of the pore is L, and the electric field $E(z)$ is in the z direction. Constancy of the current I through any cross section orthogonal to the z axis requires

$$E(z) = \frac{I}{\sigma\pi[R^2(z) - a^2]}, \tag{1}$$

where σ is the ionic conductivity of the buffer. It is assumed here that the electric field and current vectors make only a small angle to the z axis, an assumption that is asymptotically approached in the limit $|R'(z)| \ll 1$ for all z where the prime indicates derivative. The electrical conductivity σ is taken as a constant in the pore with the same value as in the buffer.

---

*Electronic address: s-ghosal@northwestern.edu

[1] In the experiments reported in Ref. [14] the pore is actually pyramidal in shape, tapering to a cone near the apex. However, since most of the resistance comes from the zone with the smallest gap width, the difference is not very significant.

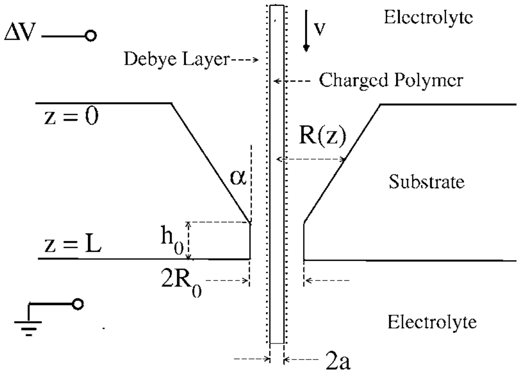

FIG. 1. Translocation of a polyelectrolyte across a nanopore, geometry of the pore region.

Next the fluid flow in the region between the polyelectrolyte cylinder and the walls of the nanopore is described, assuming that classical continuum constant density hydrodynamics is applicable. The assumption $|R'(z)| \ll 1$ immediately suggests that the problem may be treated in the lubrication limit [15,16], so that (i) the pressure (p) is independent of the radial coordinate (r), $p = p(z)$, (ii) the flow ($\mathbf{u}$) is primarily along the z axis, $\mathbf{u} \sim w(r,z)\hat{\mathbf{k}}$, and (iii) axial gradients are negligible in comparison with radial ones. Therefore, w satisfies

$$-\frac{dp}{dz} + \frac{\mu}{r}\frac{d}{dr}\left(r\frac{dw}{dr}\right) = 0, \tag{2}$$

where μ is the dynamic viscosity of the buffer. Equation (2) does not contain an electric body force term because, except for a thin Debye layer next to the polyelectrolyte, the bulk solution is electrically neutral.

In order to solve Eq. (2) boundary conditions must now be specified. On the pore walls the classical boundary condition of *no slip* is assumed:

$$w(R(z),z) = 0. \tag{3}$$

The polyelectrolyte cylinder itself will be surrounded by a charge cloud of counter-ions. The thickness of this Debye layer is measured by the Debye length λ_D, which for the high salt ($\sim$1 M KCl) buffers in these experiments is extremely small: $\lambda_D \sim 0.3$ nm. The problem is therefore treated in the thin-Debye-layer limit, which amounts to prescribing an apparent slip [17,18] on charged surfaces (in SI units):

$$w(a,z) - v = -\frac{\epsilon \zeta E(z)}{\mu}. \tag{4}$$

Here v is the translocation velocity of the polyelectrolyte, ζ is the zeta potential at the surface of the polyelectrolyte, and ϵ is the permittivity of the electrolyte. The boundary condition (4) provides the coupling between the fluid and electrical problems.

The solution to Eq. (2) with boundary conditions (3) and (4) is

$$w(r,z) = -\frac{p'(z)}{4\mu}(R^2 - r^2) + \left\{ v + \frac{a^2}{R^2 - a^2}u_e + \frac{p'(z)}{4\mu}(R^2 - a^2)\right\}\frac{\ln(R/r)}{\ln(R/a)}, \tag{5}$$

where

$$u_e = -\frac{\epsilon \zeta I}{\pi a^2 \sigma \mu} \tag{6}$$

defines a characteristic velocity scale for the problem. The pressure gradient $p'(z)$ can be determined from the condition of mass conservation,

$$Q = \int_a^{R(z)} w(r,z)(2\pi r)dr, \tag{7}$$

where Q is the flow rate through the pore. Substitution of Eq. (5) into Eq. (7) gives

$$\frac{a^2}{4\mu}\frac{dp}{dz} = \frac{Q}{\pi a^2}\frac{2\ln R_*}{(R_*^2 - 1)f} - \left(v + \frac{u_e}{R_*^2 - 1}\right)\frac{R_*^2 - 2\ln R_* - 1}{(R_*^2 - 1)f}, \tag{8}$$

where $f = R_*^2 - 1 - (R_*^2 + 1)\ln R_*$ and $R_* = R(z)/a$. The solutions (5) and (8) still contains two undetermined parameters v and Q. These are determined by imposing the conditions that there be no pressure difference across the pore,

$$p(0) = p(L), \tag{9}$$

and that the total force on the polyelectrolyte (which includes its Debye layer) is zero:

$$\int_0^L 2\pi a \mu \left.\frac{\partial w}{\partial r}\right|_{r=a} dz = 0. \tag{10}$$

The total force is zero since the polyelectrolyte moves through the pore without acceleration.

Equations (9) and (10) yield, after some algebra,

$$\frac{Q}{\pi a^2 u_e} = \frac{I_0 I_2 - I_1 I_3}{I_1 I_2 + 2 I_0 I_2 - I_0 I_1}, \tag{11}$$

$$\frac{v}{u_e} = \frac{I_0^2 - 2 I_0 I_3 - I_0 I_2}{I_1 I_2 + 2 I_0 I_2 - I_0 I_1}, \tag{12}$$

where I_0, I_1, I_2, and I_3 are dimensionless constants that depend solely on pore shape. They are defined as follows: $I_0 = \langle f^{-1}\rangle$, $I_1 = \langle f^{-1}(R_*^2 - 1)\rangle$, $I_2 = \langle f^{-1}(R_*^2 - 1)^{-1}(R_*^2 - 2\ln R_* - 1)\rangle$, and $I_3 = \langle f^{-1}(R_*^2 - 1)^{-2}(R_*^2 - 2\ln R_* - 1)\rangle$, where $\langle \cdots \rangle = L^{-1}\int_0^L (\cdots) dz$ denotes average along the pore length.

To calculate a numerical value for the translocation speed (v) from Eq. (12), the ζ potential in Eq. (6) must be related to the charge per unit length of the polyelectrolyte, λ, which is usually known from the chemistry. In order to do so, one must adopt some model for the structure of the Debye layer. For the purpose of this calculation, the simplest model should suffice. Thus, it is assumed that the Debye layer is

TABLE I. Experimental parameters from Ref. [14].

R_0 (nm)	a (nm)	L (nm)	h_0 (nm)	α (deg)	λ_D (nm)	λ (e/nm)	ΔV (mV)
5.0/4.0	1.0	340	40	36	0.3	−5.9	−120

described by the Poisson Boltzmann equation in the Debye-Huckel limit [19]. Therefore, the electric potential due to the polyelectrolyte, $\phi(r)$, satisfies

$$\frac{1}{r}\frac{d}{dr}\left(r\frac{d\phi}{dr}\right)=\frac{\phi}{\lambda_D^2}, \tag{13}$$

with the boundary conditions $\phi(a)=\zeta$ and $\phi(\infty)=0$. The solution to this boundary value problem may be expressed in terms of the zeroth-order modified Bessel function K_0:

$$\phi(r)=\frac{K_0(r/\lambda_D)}{K_0(a/\lambda_D)}\zeta. \tag{14}$$

The linear charge density λ can be related to the potential ϕ by Gauss's law:

$$-2\pi a\phi'(a)=\frac{\lambda}{\epsilon}. \tag{15}$$

Evaluating $\phi'(a)$ from Eq. (14) and substituting into Eq. (15) we have

$$\zeta=\frac{\lambda\lambda_D}{2\pi a\epsilon}\frac{K_0(a/\lambda_D)}{K_1(a/\lambda_D)}, \tag{16}$$

where K_1 is the modified Bessel function of order 1. For the purpose of comparison with experimental data, it is convenient to replace the current I in Eq. (6) with the potential difference across the pore, $\Delta V=V(0)-V(L)$, where $V(z)$ is the externally applied potential in the pore. Such a relation (Ohm's law) is readily obtained on integrating Eq. (1) between $z=0$ and $z=L$: $I/(\pi\sigma a^2)=\Delta V/(I_4L)$ where $I_4=\langle(R_*^2-1)^{-1}\rangle$. Therefore Eq. (6) for u_e may be written in an alternate form that does not involve the current or the conductivity,

$$u_e=-\frac{\epsilon\zeta}{\mu}\frac{\Delta V}{L}\frac{1}{I_4}=-\frac{u_{e0}}{I_4}. \tag{17}$$

The quantity $u_{e0}=(\epsilon\zeta/\mu)(\Delta V/L)$ has a very simple interpretation: it is the velocity with which a particle of any shape and the surface potential ζ will move if placed in an unbounded fluid medium and acted upon by the average electric field that exists within the pore [20]. The funnel shape shown in Fig. 1 may be assumed for the solid-state nanopores: $R(z)=R_0+(L-h_0-z)\tan\alpha$ if $z<L-h_0$ and $R(z)=R_0$ otherwise, α being the semivertical angle of the cone. The integrals I_0, I_1, I_2, I_3, and I_4 are then evaluated numerically.

The prediction for the translocation speed v given by Eq. (12) is now compared with a set of measured values reported by Storm *et al.* [4,14]. Table I summarizes the various parameters needed for such a comparison (e is the charge of a proton). The pore radius $R_0=4.0$ nm for the experiment with circular DNA (see Fig. 2) but 5.0 nm in all other cases. The dielectric constant $\epsilon/\epsilon_0=80$ and dynamic viscosity $\mu=8.91\times10^{-4}$ Pa s for the electrolyte are taken as those of water. Equation (16) then gives[2] $\zeta\approx-56$ mV. For highly charged polyelectrolytes such as DNA, it has been shown by Manning [21] and Oosawa [22] that some of the counter-ions condense onto the surface of the polyelectrolyte, reducing its effective charge to $\lambda_{\mathrm{eff}}=\lambda/q_B$. For DNA, at room temperature, in weak salt solutions ($\lambda_D\gg a$) and away from boundaries, the Manning factor $q_B\approx4.2$. However, under the conditions of the experiment, $\lambda_D\sim a$, and further, the polyelectrolyte is in the vicinity of a dielectric/conductor interface which has an effect on q_B [23]. Thus, the value of ζ is uncertain by perhaps as much as an order of magnitude. The characteristic velocity u_{e0} defined by Eq. (17) is $u_{e0}\approx15.7$ mm/s in the absence of counter-ion condensation ($q_B=1$) but it is reduced to 3.7 mm/s if $q_B=4.2$ is assumed.

The lines in Fig. 2 show the translocation velocity v calculated from Eq. (12) as a function of $R_0/a-1$. The experimental data points are determined using Table I and Fig. 11 of Ref. [14]. The translocation velocities are obtained by dividing the DNA length (11.5 kbp and 48.5 kbp) by the measured mean translocation times. The uncertainty in the velocity corresponds to the spread in the translocation times. Four different modes can be distinguished [14] for the DNA crossing, the two fundamental modes denoted as types 1 and 2 and the mixed-mode types 12 and 21. In type 1 the DNA passes through the nanopore without any folds. In the case of type-2 translocation of a linear chain or in the translocation of a circular chain, the DNA is folded in half so that its effective length is reduced to $L/2$ from L. In that case the two parallel DNA fibers that simultaneously thread the pore may be regarded as equivalent to a single cylindrical polyelectrolyte which has the same ζ potential but a larger radius a_{eff}. The effective radius is determined by the requirement that the same fractional area of the pore be blocked. That is, the effective radius is $a_{\mathrm{eff}}=\sqrt{2}a\approx1.41$ nm. Such a reduction has been used to calculate $R_0/a-1$ for the type-2 and circular DNA cases shown in Fig. 2. An uncertainty of ±0.5 nm for the value of R_0 is assumed due to errors such as the departure of the nanopore from a strictly circular shape and possible presence of hydration shells on the surface.

Lubensky and Nelson [5] and Storm *et al.* [24] estimated the viscous force as $f_v\sim(2\pi aL\mu v)/(R_0-a)\sim0.5-5.0$ pN, if $v\sim1-10$ mm/s. When compared with the electrical force $f_{el}\sim\lambda\Delta V\sim113$ pN, it appeared that viscous friction could not balance the electrical traction and therefore other mechanisms were needed to explain the observed translocation rates. Figure 2 demonstrates that this is not so. Two effects intervene to lower the estimate for the electrical force and raise the estimate for the viscous force: (a) due to shielding by counter-ions, the electrical force is reduced by as much as an order of magnitude [25] and (b) the change in the flow velocity takes place primarily across the thickness of a

---

[2] A ζ potential also exists on the substrate-electrolyte interface, but at the very high counter-ion concentrations considered here (~1 M) its value is negligibly small compared to that of the polyelectrolyte (Ref. [29]).

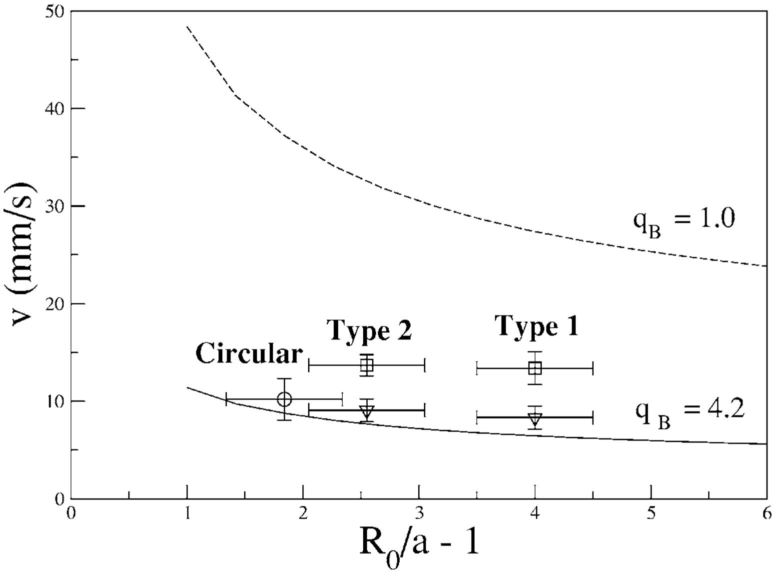

FIG. 2. Translocation velocity (v) as a function of the dimensionless gap width ($R_0/a-1$) in the case of 11.5 kbp dsDNA (squares), 48.5 kbp dsDNA (triangles), and 11.5 kbp circular dsDNA (circle). Lines are the predictions from the model (a) assuming counter-ion condensation in accordance with the Manning theory for a line charge (solid line) and (b) ignoring counter-ion condensation (dashed line).

Debye layer, λ_D, and not over R_0-a, so that the actual viscous force is larger by a factor of approximately $(R_0-a)/\lambda_D \sim 10$. In fact, in the thin-Debye-layer limit, the solution for the fluid flow within the Debye layer guarantees an exact cancellation of the electrical force with the viscous force on every surface element dS of the polyelectrolyte. Figure 2 also shows that the translocation velocity does have a weak dependence on polymer length. In a certain range of polymer lengths, the data can be fit by a power law $v \sim L^{-0.26}$ [24]. This fact cannot be explained by the model presented here or by any other model that localizes all of the resistive force within the pore. The dependence on polymer length must arise from additional effects not considered here such as the viscous resistance from the part of the polymer that lies outside the pore [24].

The largest source of uncertainty in the above calculation arises from the difficulty of obtaining accurately a value of ζ. The current understanding of the physics of the Debye layer is still incomplete so that even in the classical problems of electrokinetics, such as in the electrophoresis of a sphere, unresolved discrepancies exist between Eq. (4) and the ζ determined from more direct measurements of charge [26]. The use of the lubrication equations and the assumption of a simplified axisymmetric geometry for the pore also contribute to the error but these are likely to be much less than the ones just mentioned. One may question the use of continuum hydrodynamics in the first place to calculate the mean motion of the polymer. Note, however, in the case of water, the intermolecular spacing is of the order of 0.1 nm which is significantly smaller than the ~2 nm inner diameter and 4–5 nm outer diameter of the pore. The applicability of the no-slip condition at the solid-liquid interfaces is still a matter of contention [27]. Nevertheless, possible slip lengths are miniscule and amount to an uncertainty in the values of R_0 and a by perhaps a fraction of a nanometer. In fact, classical hydrodynamics (i.e., Stokes equations with no-slip boundary conditions) works reasonably well for water down to several tenths of nanometers; for example, for nonelectrolytes, molecular sizes calculated on the basis of the Stokes-Einstein relation or Einstein's viscosity law for dilute suspensions agree with molecular-structure-based determinations to within 10%–15% [28] even for molecules in the 0.3–0.5 nm range. The use of the continuum hydrodynamics model for calculating statistical averages in the manner used here is therefore not likely to be a significant source of uncertainty, at least for the solid-state nanopores.

In summary, a model of the pore resistance based on continuum hydrodynamics and electrostatics produces estimates for the translocation speed of dsDNA in solid-state nanopores to within an order of magnitude of experimental values. The present analysis needs to be modified for protein nanopores because certain approximations such as the thin Debye layer are not applicable in that case.

The author wishes to thank Professor David Deamer for helpful discussions.

---

[1] J. Kasianowicz, E. Brandin, D. Branton, and D. Deamer, Proc. Natl. Acad. Sci. U.S.A. **93**, 13770 (1996).
[2] A. Meller *et al.*, Proc. Natl. Acad. Sci. U.S.A. **97**, 1079 (2000).
[3] W. Vercoutere *et al.*, Nat. Biotechnol. **19**, 248 (2001).
[4] A. Storm *et al.*, Nat. Mater. **2**, 537 (2003).
[5] D. Lubensky and D. Nelson, Biophys. J. **77**, 1824 (1999).
[6] M. Muthukumar, Phys. Rev. Lett. **86**, 3188 (2001).
[7] W. Sung and P. J. Park, Phys. Rev. Lett. **77**, 783 (1996).
[8] R. Boehm, Macromolecules **32**, 7645 (1999).
[9] M. Muthukumar, J. Chem. Phys. **111**, 10371 (1999).
[10] M. Muthukumar, J. Chem. Phys. **118**, 5174 (2003).
[11] K. K. Kumar and K. L. Sebastian, Phys. Rev. E **62**, 7536 (2000).

[12] S. K. Lee and W. Sung, Phys. Rev. E **63**, 021115 (2001).

[13] K. L. Sebastian and A. K. R. Paul, Phys. Rev. E **62**, 927 (2000).

[14] A. J. Storm, J. H. Chen, H. W. Zandbergen, and C. Dekker, Phys. Rev. E **71**, 051903 (2005).

[15] G. Batchelor, *An Introduction to Fluid Dynamics* (Cambridge University Press, Cambridge, England, 2000).

[16] S. Ghosal, J. Fluid Mech. **459**, 103 (2002).

[17] H. Helmholtz, Ann. Phys. Chem. **7**, 337 (1879).

[18] M. Smoluchowski, Bull. Int. Acad. Sci. Cracovie **8**, 182 (1903).

[19] W. Russel, D. Saville, and W. Schowalter, *Colloidal Dispersions* (Cambridge University Press, Cambridge, England, 1989).

[20] F. Morrison, Jr., J. Colloid Interface Sci. **34**, 45 (1970).

[21] G. Manning, J. Chem. Phys. **51**, 924 (1969).

[22] F. Oosawa, *Polyelectrolytes* (Marcel Dekker, New York, 1971).

[23] T. Tang, A. Jagota, and C. Hui, J. Colloid Interface Sci. **299**, 564 (2006).

[24] A. Storm *et al.*, Nano Lett. **5**, 1193 (2005).

[25] Y. Rabin and M. Tanaka, Phys. Rev. Lett. **94**, 148103 (2005).

[26] Y. Kim and R. Netz, J. Chem. Phys. **124**, 114709 (2006).

[27] E. Lauga, M. P. Brenner, and H. A. Stone, in *Handbook of Experimental Fluid Dynamics*, edited by J. Foss, C. Tropea, and A. Yarin (Springer, New York, 2006), Chap. 15.

[28] S. G. Schultz and A. K. Solomon, J. Gen. Physiol. **44**, 1189 (1961).

[29] B. Kirby and E. Hasselbrink, Electrophoresis **25**, 187 (2004).